

# Theory for transport through a single magnetic molecule: endohedral N@C<sub>60</sub>

Florian Elste\* and Carsten Timm†

Institut für Theoretische Physik, Freie Universität Berlin, Arnimallee 14, D-14195 Berlin, Germany

(Dated: October 25, 2004)

We consider transport through a single N@C<sub>60</sub> molecule, weakly coupled to metallic leads. Employing a density-matrix formalism we derive rate equations for the occupation probabilities of many-particle states of the molecule. We calculate the current-voltage characteristics and the differential conductance for N@C<sub>60</sub> in a break junction. Our results reveal Coulomb-blockade behavior as well as a fine structure of the Coulomb-blockade peaks due to the exchange coupling of the C<sub>60</sub> spin to the spin of the encapsulated nitrogen atom.

PACS numbers: 75.50.Xx, 85.65.+h

The rapid progress of miniaturization of electronic devices has lead to chip features smaller than 100 nm, for which standard semiconductor technology reaches its limit. One proposed solution is a transistor consisting of a single molecule. In recent years transport through single molecules has been studied quite extensively,<sup>1,2,3,4,5,6</sup> for example in break junctions.<sup>7,8,9</sup> *Inelastic* transport occurs due to the interaction of electrons with internal vibrational or magnetic degrees of freedom of the molecules. Transport through magnetic molecules<sup>10,11,12</sup> is particularly interesting also from the point of view of *spintronics*, i.e., the idea of exploiting the electron spin in electronic devices. While most molecules are normally non-magnetic, there are exceptions such as endohedral N@C<sub>60</sub>, i.e., a nitrogen atom encapsulated in a C<sub>60</sub> cage.<sup>13</sup> It is known that the encapsulated atom retains its p-electrons,<sup>13</sup> leading to a localized spin  $S_N = 3/2$ . There are fascinating ideas of employing this spin in a quantum computer.<sup>14</sup>

In this paper we propose to measure the current through a single N@C<sub>60</sub> molecule in a break junction and we calculate the current-voltage (*IV*) characteristics and the differential conductance  $dI/dV$ . Since transport through a single C<sub>60</sub> molecule has been demonstrated<sup>8</sup> and the synthesis of endohedral fullerenes is also feasible,<sup>13</sup> such an experiment is possible with present-day apparatus. Besides the typical Coulomb blockade behavior we predict a characteristic fine structure of the Coulomb blockade peaks in  $dI/dV$  due to the exchange coupling of the C<sub>60</sub> spin to the spin 3/2 of the encapsulated nitrogen atom. It should be mentioned that the discussion of transport through P@C<sub>60</sub> proceeds quite analogously and yields qualitatively identical results.

In our model the N@C<sub>60</sub> molecule is treated as a quantum dot and the leads, labeled as L (left) and R (right), as macroscopic charge reservoirs. As C<sub>60</sub> generally prefers to be singly or doubly negatively charged,<sup>15</sup> we assume that electronic transport through the molecule involves only the three-fold degenerate LUMO (lowest unoccupied molecular orbital), whereas the five-fold degenerate HOMO (highest occupied molecular orbital) remains fully occupied.<sup>16</sup> Charge transfer from the nitrogen atom to the fullerene cage is assumed to be negligible. When the LUMO is partially occupied, the net spin of the electrons in the LUMO,  $\mathbf{S}_{C_{60}}$ , couples to the spin 3/2 of the nitrogen atom,  $\mathbf{S}_N$ , and the total spin of

the molecule is  $\mathbf{S} = \mathbf{S}_{C_{60}} + \mathbf{S}_N$ . Relaxation in the leads is assumed to be sufficiently fast so that the electron distributions in the leads can be described by Fermi functions. The full Hamiltonian of the system is  $H = H_d + H_{\text{leads}} + H_t$ , where

$$H_d = (\varepsilon - eV_g) n_d + \frac{U}{2} n_d(n_d - 1) - J \mathbf{S}_{C_{60}} \cdot \mathbf{S}_N \quad (1)$$

represents the molecular quantum dot,

$$H_{\text{leads}} = \sum_{\alpha=L,R} \sum_{\mathbf{k}\sigma} \epsilon_{\alpha\mathbf{k}} a_{\alpha\mathbf{k}\sigma}^\dagger a_{\alpha\mathbf{k}\sigma} \quad (2)$$

represents the leads, and

$$H_t = \sum_{\alpha=L,R} \sum_{n\sigma\mathbf{k}} (t_{\alpha} a_{\alpha\mathbf{k}\sigma}^\dagger c_{n\sigma} + t_{\alpha}^* c_{n\sigma}^\dagger a_{\alpha\mathbf{k}\sigma}) \quad (3)$$

describes the tunneling between the dot and the leads, which is assumed to be weak. Here, the operator  $c_{n\sigma}^\dagger$  creates an electron with spin  $\sigma$  in the molecular orbital  $n$ , while  $a_{\alpha\mathbf{k}\sigma}^\dagger$  creates an electron in lead  $\alpha$  with spin  $\sigma$ , momentum  $\mathbf{k}$  and energy  $\epsilon_{\alpha\mathbf{k}}$  relative to the Fermi energy.  $n_d = \sum_{n\sigma} c_{n\sigma}^\dagger c_{n\sigma}$  and  $\mathbf{S}_{C_{60}} = \sum_{n\sigma\sigma'} c_{n\sigma}^\dagger (\boldsymbol{\sigma}_{\sigma\sigma'}/2) c_{n\sigma'}$  are the number and spin operators of electrons on the dot, respectively. Electron-electron interaction is taken into account by the local Coulomb repulsion  $U$  and the exchange interaction with the nitrogen spin by the exchange coupling  $J$ . The values of  $\varepsilon$ ,  $U$  and  $J$  are not well known at present. *Ab-initio* calculations indicate that C<sub>60</sub><sup>2-</sup> is slightly bound relative to C<sub>60</sub><sup>-</sup>.<sup>15</sup> For our numerical calculations we use  $\varepsilon = -2.7$  eV and  $U = 2.5$  eV.<sup>15,17</sup>  $J$  appears to be *ferromagnetic*. We take  $J = 1$  meV from *ab-initio* calculations of Udvardi.<sup>18</sup> Note that the exchange coupling is significantly smaller than the energy of relevant vibrational modes. The oscillations of the molecule as a whole have an energy of the order of 5 meV.<sup>8</sup> The oscillations of the nitrogen atom within the C<sub>60</sub> have an energy of 13 meV,<sup>19</sup> whereas the modes of the C<sub>60</sub> cage lie at much higher energies.

We next derive rate equations for this model starting from the equation of motion for the density matrix  $\rho$ ,<sup>5,6,20</sup>  $d\rho_I(t)/dt = -i [H_{tI}, \rho_I(t)]$ . Here, the index  $I$  denotes the interaction representation with respect to  $H_t$ . Integration and

iteration gives<sup>5,20</sup>

$$\begin{aligned} \frac{d\rho_I(t)}{dt} = & -i [H_{tI}(t), \rho_I(0)] \\ & - \int_0^t dt' [H_{tI}(t), [H_{tI}(t'), \rho_I(t')]]. \end{aligned} \quad (4)$$

Assuming that the leads are weakly affected by the quantum dot and neglecting correlations between the two,  $\rho_I(t)$  can be replaced by the direct product of the *reduced density matrix* of the dot,  $\rho_{dI}(t) \equiv \text{Tr}_{\text{leads}} \rho_I(t)$ , and the density matrix  $\rho_{\text{leads}}$  of the leads,  $\rho_I(t) \approx \rho_{dI}(t) \otimes \rho_{\text{leads}}$ . We then obtain

$$\frac{d\rho_{dI}(t)}{dt} = - \int_0^t dt' \text{Tr}_{\text{leads}} [H_{tI}(t), [H_{tI}(t'), \rho_{dI}(t') \otimes \rho_{\text{leads}}]]. \quad (5)$$

Returning to the Schrödinger representation and using the Markov approximation<sup>5,20</sup>  $\rho_{dI}(t') \approx \rho_{dI}(t)$ , we find

$$\begin{aligned} \frac{d\rho_d(t)}{dt} = & -i [H_d, \rho_d] - \text{Tr}_{\text{leads}} \int_0^\infty dt' [H_t, \\ & [e^{-i(H_d+H_{\text{leads}})t'} H_t e^{i(H_d+H_{\text{leads}})t'}, \rho_d(t) \otimes \rho_{\text{leads}}]] \end{aligned} \quad (6)$$

as the equation of motion for  $\rho_d$ . This expression shows that the tunneling Hamiltonian  $H_t$  is treated in second-order perturbation theory. Taking the trace over the degrees of freedom of the leads produces Fermi functions according to

$$\text{Tr}_{\text{leads}} \rho_{\text{leads}} a_{\alpha\mathbf{k}\sigma}^\dagger a_{\alpha'\mathbf{k}'\sigma'} = \delta_{\alpha\alpha'} \delta_{\mathbf{k}\mathbf{k}'} \delta_{\sigma\sigma'} f(\epsilon_{\alpha\mathbf{k}} - \mu_\alpha), \quad (7)$$

where  $\mu_\alpha$  denotes the chemical potential of lead  $\alpha$  due to the applied source-drain voltage  $V$ . Expanding the nested commutators in Eq. (6) and inserting Eq. (3) gives eight terms,

$$\begin{aligned} \frac{d\rho_d(t)}{dt} = & - \int_0^\infty dt' \sum_{\alpha n n' \sigma \mathbf{k}} |t_\alpha|^2 \\ & \times \left\{ f(\epsilon_{\alpha\mathbf{k}} - \mu_\alpha) e^{i\epsilon_{\alpha\mathbf{k}} t'} c_{n\sigma} e^{-iH_d t'} c_{n'\sigma}^\dagger e^{iH_d t'} \rho_d(t) \right. \\ & + [1 - f(\epsilon_{\alpha\mathbf{k}} - \mu_\alpha)] e^{-i\epsilon_{\alpha\mathbf{k}} t'} c_{n\sigma}^\dagger e^{-iH_d t'} c_{n'\sigma} e^{iH_d t'} \rho_d(t) \\ & - [1 - f(\epsilon_{\alpha\mathbf{k}} - \mu_\alpha)] e^{i\epsilon_{\alpha\mathbf{k}} t'} c_{n\sigma} \rho_d(t) e^{-iH_d t'} c_{n'\sigma}^\dagger e^{iH_d t'} \\ & - f(\epsilon_{\alpha\mathbf{k}} - \mu_\alpha) e^{-i\epsilon_{\alpha\mathbf{k}} t'} c_{n\sigma}^\dagger \rho_d(t) e^{-iH_d t'} c_{n'\sigma} e^{iH_d t'} \\ & - [1 - f(\epsilon_{\alpha\mathbf{k}} - \mu_\alpha)] e^{-i\epsilon_{\alpha\mathbf{k}} t'} e^{-iH_d t'} c_{n\sigma} e^{iH_d t'} \rho_d(t) c_{n'\sigma}^\dagger \\ & - f(\epsilon_{\alpha\mathbf{k}} - \mu_\alpha) e^{i\epsilon_{\alpha\mathbf{k}} t'} e^{-iH_d t'} c_{n\sigma}^\dagger e^{iH_d t'} \rho_d(t) c_{n'\sigma} \\ & + f(\epsilon_{\alpha\mathbf{k}} - \mu_\alpha) e^{-i\epsilon_{\alpha\mathbf{k}} t'} \rho_d(t) e^{-iH_d t'} c_{n\sigma} e^{iH_d t'} c_{n'\sigma}^\dagger \\ & \left. + [1 - f(\epsilon_{\alpha\mathbf{k}} - \mu_\alpha)] e^{i\epsilon_{\alpha\mathbf{k}} t'} \rho_d(t) e^{-iH_d t'} c_{n\sigma}^\dagger e^{iH_d t'} c_{n'\sigma} \right\}. \end{aligned} \quad (8)$$

The probability of the dot being in the many-particle state  $|n\rangle$  is  $P^n \equiv \langle n | \rho_d(t) | n \rangle$ . Introducing the overlap matrix elements  $C_{mn}^\sigma \equiv \langle m | \sum_i c_{i\sigma} | n \rangle$  and  $C_{mn}^{\sigma\dagger} \equiv \langle m | \sum_i c_{i\sigma}^\dagger | n \rangle$  and identifying the integrals in Eq. (8) as delta functions we can write Eq. (8) as a set of rate equations

$$\frac{dP^n}{dt} = \sum_{m \neq n} P^m R_{m \rightarrow n} - P^n \sum_{m \neq n} R_{n \rightarrow m} \quad (9)$$

with transition rates

$$\begin{aligned} R_{n \rightarrow m} = & \sum_{\alpha\sigma} 2\pi |t_\alpha|^2 N_\alpha f(\epsilon_m^d - \epsilon_n^d - \mu_\alpha) \\ & \times (|C_{nm}^\sigma|^2 + |C_{mn}^\sigma|^2). \end{aligned} \quad (10)$$

Here,  $\epsilon_n^d$  is the energy of the many-particle state  $|n\rangle$  of the dot and  $N_\alpha$  denotes the density of states of lead  $\alpha$ , which we take to be constant and equal for both leads. The matrix elements  $C_{mn}^\sigma$  ( $C_{mn}^{\sigma\dagger}$ ) can only be finite if the electron number of state  $|n\rangle$  is larger (smaller) by one than the electron number of state  $|m\rangle$ . We are interested in the *stationary state*, which corresponds to  $dP^n/dt = 0$  for all states  $|n\rangle$ .

In deriving Eq. (9) we have assumed that the density matrix  $\rho_d$  is *completely diagonal*. This assumption requires some thought since many of the eigenstates of our molecular quantum dot are degenerate so that one might expect finite off-diagonal components even in the stationary state. However, this is not the case: Let  $U$  be a unitary matrix that leaves the dot Hamiltonian  $H_d$  invariant. With any stationary density matrix  $\rho_d$ ,  $U\rho_d U^\dagger$  is another solution. Now suppose that there exists a stationary solution  $\rho_d$  that is *not* diagonal within a block of degenerate states. Then one can choose  $U$  so that  $U\rho_d U^\dagger$  is diagonal since the nonzero off-diagonal components have been assumed to connect degenerate states (we exclude the case of accidental degeneracy). But then  $U\rho_d U^\dagger$  has *unequal* diagonal components, i.e., probabilities  $P^n$ , for symmetry-related states. This is clearly unphysical. On the other hand, if  $\rho_d$  is already diagonal with degenerate dot states having equal diagonal components, any allowed transformation  $U$  leaves  $\rho_d$  invariant.

The current operator for lead  $\alpha$  reads<sup>21</sup>

$$I_\alpha = i [H, N_\alpha] = -i \sum_{n\sigma\mathbf{k}} (t_\alpha c_{n\sigma}^\dagger a_{\alpha\mathbf{k}\sigma} - t_\alpha^* a_{\alpha\mathbf{k}\sigma}^\dagger c_{n\sigma}). \quad (11)$$

Tracing out the leads we arrive at an expression for the expectation value of the current,

$$\begin{aligned} \langle I_\alpha \rangle = & 2\pi N_\alpha |t_\alpha|^2 \sum_{ml\sigma} \left( f(\epsilon_l^d - \epsilon_m^d - \mu_\alpha) |C_{ml}^\sigma|^2 \right. \\ & \left. - [1 - f(\epsilon_m^d - \epsilon_l^d - \mu_\alpha)] |C_{lm}^\sigma|^2 \right) P^m. \end{aligned} \quad (12)$$

We here consider the symmetric case  $t_L = t_R$  and  $\mu_L = -\mu_R = V/2$ .

As there are  $\binom{6}{i}$  possible ways of filling the three-fold degenerate  $C_{60}$  LUMO with  $i$  electrons according to the Pauli principle and as the nitrogen atom possesses a spin 3/2, solving the rate equations and calculating the current reduces to an eigenvalue problem of dimension  $4 \times \sum_{i=0}^6 \binom{6}{i} = 256$ .

Our numerical results show that the current  $I$  is symmetric with respect to the applied source-drain voltage  $V$  in accordance with the high symmetry of the fullerene molecule. The  $IV$  characteristics plotted in Fig. 1 show a conductance gap for  $|V| < 0.4$  V due to Coulomb blockade. Each step in the main  $IV$  curve corresponds to the opening of additional current channels. Simultaneously, the average occupation  $\langle n \rangle$  of the dot changes. For the parameters chosen

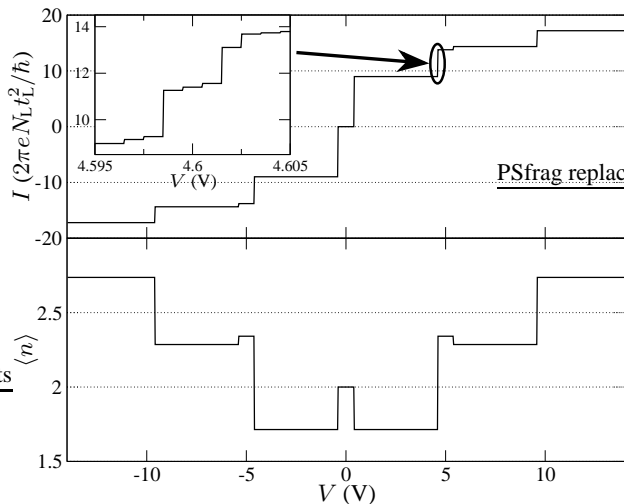


FIG. 1: Current  $I$  and average occupation  $\langle n \rangle$  of the  $C_{60}$  LUMO as a function of the source-drain voltage  $V \equiv \mu_L - \mu_R$  for  $\varepsilon = -2.7$  eV,  $U = 2.5$  eV,  $J = 1$  meV,  $V_g = 0$  V and  $T = 0.01$  K. The inset shows the fine structure of one particular Coulomb-blockade step.

above, the  $C_{60}^{2-}$  state is the ground state.<sup>15</sup> At the first step, the potential drop becomes large enough to allow transitions between the charge states  $-2$  and  $-1$ , as the chemical potential  $\mu_L = V/2$  reaches the value assumed for the ionization energy  $E(C_{60}^{2-}) - E(C_{60}^-) = \varepsilon + U = -0.2$  eV. At the second step, transitions between the charge states  $-2$  and  $-3$  become possible, etc.

Our results for the occupation probabilities reveal that detailed balance is satisfied for the broad plateaus in Fig. 1, i.e.,  $P^n R_{n \rightarrow m} = P^m R_{m \rightarrow n}$ . As a consequence, the dot occupation probabilities  $P^n$  for all *occupied* states are identical in the limit  $T \rightarrow 0$ , as the transition rates  $R_{n \rightarrow m}$  are symmetric for each pair  $n, m$  of occupied states. This also accounts for the fact that the average occupation  $\langle n \rangle$  is exactly 2 for  $V = 0$  V, decreases to  $(24 \times 1 + 60 \times 2)/(24 + 60) = 12/7 \approx 1.71$  at the first step, when the molecule is in one of 24 singly charged or 60 doubly charged states with equal probability, and increases to  $(24 \times 1 + 60 \times 2 + 80 \times 3)/(24 + 60 + 80) = 96/41 \approx 2.34$  at the second step, when 80 additional states become available. Furthermore, we find that each Coulomb-blockade step shows a characteristic fine structure, which we discuss below.

The calculation of the differential conductance  $dI/dV$  as a function of source-drain voltage  $V$  and gate voltage  $V_g$  shows the usual *Coulomb diamonds*, see Fig. 2. Close to the degeneracy points between different charge states we observe a relatively complex fine structure, corresponding to the steps in the inset of Fig. 1. We assume very low temperatures,  $k_B T \ll J$ , to exhibit the structure more clearly. At higher temperatures the peaks in  $dI/dV$  are thermally broadened. In the following, we briefly explain the physics behind the fine structure, taking Fig. 2(a) as an example.

Since the  $C_{60}$  spin  $S_{C_{60}}$ , the spin of the nitrogen atom,  $S_N$ , and the total spin  $S$  (where  $S = |S_{C_{60}} - S_N|, \dots, S_{C_{60}} + S_N$ )

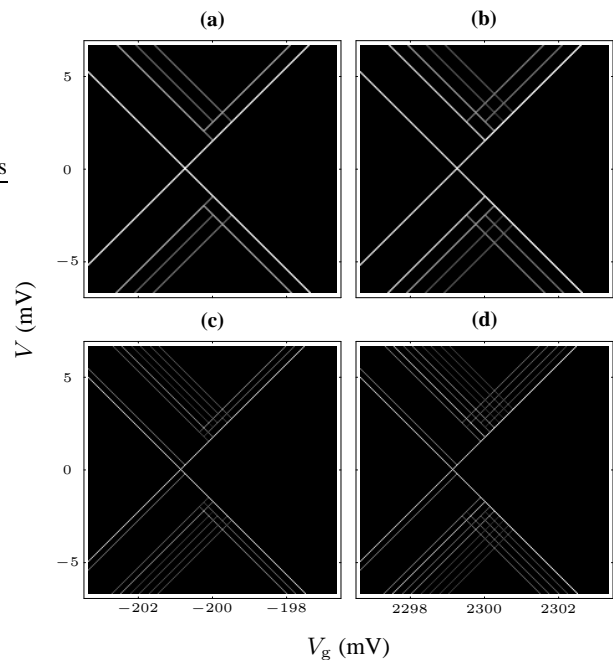


FIG. 2: Gray-scale plots of the differential conductance  $dI/dV$  as a function of source-drain voltage  $V$  and gate voltage  $V_g$  for  $T = 0.01$  K. Shown are two particular ranges of gate voltages close to the degeneracy points between charge states  $-1$  and  $-2$  (a,c) and between  $-2$  and  $-3$  (b,d). (a) and (b) show result for vanishing magnetic field and (c) and (d) for  $B = 2$  T.

are good quantum numbers, the exchange energy is

$$E_{\text{exc}} = -\frac{J}{2} [S(S+1) - S_{C_{60}}(S_{C_{60}}+1) - S_N(S_N+1)], \quad (13)$$

which leads to the level splitting illustrated in Fig. 3. The structure in Fig. 2(a) arises from transitions between charge states  $-1$  and  $-2$ , taking spin excitations into account. In equilibrium ( $V = 0$  V) only the ground state of the dot is occupied, which is the  $C_{60}^-$  state with  $S_{C_{60}} = 1/2$  and  $S = 2$  for  $V_g$  smaller than the degeneracy point  $V_g^0$  and the  $C_{60}^{2-}$  state with  $S_{C_{60}} = 1$  and  $S = 5/2$  for  $V_g > V_g^0$ , cf. Fig. 3(a). For  $V_g < V_g^0$  the *first* peak in  $dI/dV$  at nonzero  $V$  originates from the transition with  $S_{C_{60}} = 1/2 \rightarrow 1$  and  $S = 2 \rightarrow 5/2$ , corresponding to a gain of exchange energy of  $\Delta E_{\text{exc}} = -0.75$  meV. The *second* peak results from a transition with  $S_{C_{60}} = 1/2 \rightarrow 0$ ,  $S = 2 \rightarrow 3/2$  and  $\Delta E_{\text{exc}} = +0.75$  meV. Simultaneously, the transitions with  $S_{C_{60}} = 1/2 \rightarrow 0$ ,  $S = 1 \rightarrow 3/2$ ,  $\Delta E_{\text{exc}} = -1.25$  meV and  $S_{C_{60}} = 1/2 \rightarrow 1$ ,  $S = 1 \rightarrow 3/2$ ,  $\Delta E_{\text{exc}} = -0.25$  meV are enabled [dashed lines in Fig. 3(a)]. Although energetically possible, these transitions are not excited at lower source-drain voltages, because the lower levels are unoccupied. The last two peaks belong to transitions with  $S_{C_{60}} = 1/2 \rightarrow 1$ ,  $S = 1 \rightarrow 1/2$ ,  $\Delta E_{\text{exc}} = +1.25$  meV and  $S = 1/2 \rightarrow 1$ ,  $S = 2 \rightarrow 3/2$ ,  $\Delta E_{\text{exc}} = +1.75$  meV. Note that the values of  $\Delta E_{\text{exc}}$  account for the level spacing.

The situation is different for  $V_g$  significantly larger than

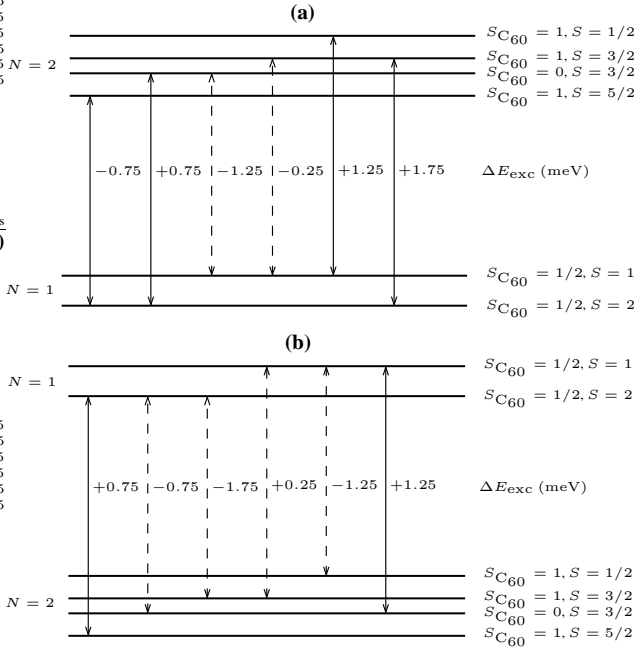


FIG. 3: Energy levels and all allowed transitions between many-particle states with one ( $N = 1$ ) and two ( $N = 2$ ) electrons, taking into account spin excitations. (a) Situation with the  $N = 1$  multiplet lower in energy than the  $N = 2$  multiplet. (b) Reverse case.

$V_g^0$ , where we observe only two peaks, cf. Fig. 2(a). As soon as the transition from the  $C_{60}^{2-}$  ground state into the lowest  $C_{60}^-$  state with  $S_{C_{60}} = 1 \rightarrow 1/2$ ,  $S = 5/2 \rightarrow 2$  and  $\Delta E_{exc} = +0.75$  meV becomes possible, the transitions corresponding to  $\Delta E_{exc} = -0.75$  meV,  $-1.75$  meV,  $+0.25$  meV, and  $-1.25$  meV [dashed lines in Fig. 3(b)] are also enabled. Again the latter four would be energetically possible at lower  $V$ , but do not appear as peaks of  $dI/dV$ , since the corresponding lower levels are unoccupied. In the vicinity of  $V_g^0$  we find that the slope of several lines abruptly changes sign. This corresponds to the situation where two levels connected in Fig. 3 by a transition cross as  $V_g$  is varied. The fine structure in Fig. 2(b) can be discussed analogously. The structure is different for all degeneracy points and can thus serve

as a *fingerprint* of the particular charge transition. This should be useful since the zero of the  $V_g$  axis is often shifted significantly from one experiment to the next.

Selection rules for single-electron tunneling require that  $\Delta S_{C_{60}} = \pm 1/2$  and  $\Delta S = \pm 1/2$ . The different brightness of the peaks in Fig. 2 is correlated with the number of transitions that are possible at a given source-drain voltage. Each allowed transition may be thought of as one current channel.

Experimentally, the *magnetic* origin of the fine structure is most conclusively tested by observing the behavior in a magnetic field. For ionized  $C_{60}$  in lattices and in solution, the orbital moment is quenched.<sup>22,23</sup> We assume that the fields generated by the electrodes in a break junction are also sufficiently strong to quench the orbital moment. Then the molecule couples to a magnetic induction  $B$  only through the *spin* moments, described by the new Hamiltonian

$$H' = H - g\mu_B B S_{C_{60}}^z - g\mu_B B S_N^z = H - g\mu_B B S^z. \quad (14)$$

Here,  $\mu_B$  is the Bohr magneton and  $g$  is the  $g$ -factor, which is  $g \approx 2$  for both the nitrogen spin  $S_N$  and the  $C_{60}$  spin. We choose a many-particle basis of simultaneous eigenstates of  $n_d$ ,  $S_{C_{60}}$ ,  $S$ , and  $S^z$ . Then the only difference is that additional Zeeman energies appear in our expression for the transition rates, Eq. (10). In Fig. 2(c,d) we show  $dI/dV$  for the same parameters as in Fig. 2(a,b) but with  $B = 2$  T. As expected, the peaks split, but in addition several peaks are absent since they are not allowed by the selection rules. For example, for  $V_g > V_g^0$  the first peak is due to a transition with  $S_{C_{60}} = 1 \rightarrow 1/2$ ,  $S = 5/2 \rightarrow 2$ , and  $N = 2 \rightarrow 1$ . Since the initial state has all spins aligned in parallel, one electron tunneling out of the dot can only reduce  $S^z$  so that there is only a *single* peak in  $dI/dV$ .

To summarize, we have presented a theory for transport through a single  $N@C_{60}$  molecule weakly coupled to metallic electrodes. Our results for the differential conductance  $dI/dV$  as a function of the source-drain and gate voltages show Coulomb blockade and exhibit a characteristic fine structure of the Coulomb-blockade peaks due to the coupling of the  $C_{60}$  spin to the spin of the encapsulated nitrogen atom.

We would like to thank W. Harneit, J. Koch, A. Mitra, and F. von Oppen for helpful discussions and the Deutsche Forschungsgemeinschaft for support through Sfb 290.

\* Electronic address: felste@physik.fu-berlin.de

† Electronic address: timm@physik.fu-berlin.de

<sup>1</sup> C. Joachim, J. K. Gimzewski, and A. Aviram, *Nature* **408**, 541 (2000).

<sup>2</sup> E. G. Emberly and G. Kirczenow, *Chem. Phys.* **281**, 311 (2002); *Phys. Rev. Lett.* **91**, 188301 (2003).

<sup>3</sup> A. Nitzan and M. A. Ratner, *Science* **300**, 1384 (2003).

<sup>4</sup> Y. Xue and M. A. Ratner, *Phys. Rev. B* **68**, 115406 (2003); **68**, 115407 (2003).

<sup>5</sup> A. Mitra, I. Aleiner, and A. J. Millis, *Phys. Rev. B* **69**, 245302 (2004).

<sup>6</sup> J. Koch and F. von Oppen, cond-mat/0409667 (unpublished).

<sup>7</sup> M. A. Reed *et al.*, *Science* **278**, 252 (1997).

<sup>8</sup> H. Park *et al.*, *Nature* **407**, 57 (2000).

<sup>9</sup> H. B. Weber *et al.*, *Chem. Phys.* **281**, 113 (2002); J. Reichert *et al.*, *Appl. Phys. Lett.* **82**, 4137 (2003).

<sup>10</sup> J. Park *et al.*, *Nature* **417**, 722 (2002).

<sup>11</sup> W. Liang *et al.*, *Nature* **417**, 725 (2002).

<sup>12</sup> C. Durkan and M. E. Welland, *Appl. Phys. Lett.* **80**, 458 (2002).

<sup>13</sup> T. Almeida Murphy *et al.*, *Phys. Rev. Lett.* **77**, 1075 (1996).

<sup>14</sup> W. Harneit, *Phys. Rev. A* **65**, 032322 (2002).

<sup>15</sup> R. L. Hettich, R. N. Compton, and R. H. Ritchie, *Phys. Rev. Lett.* **67**, 1242 (1991).

<sup>16</sup> N. Laouini, O. K. Andersen, and O. Gunnarsson, *Phys. Rev. B* **51**, 17446 (1995).

<sup>17</sup> M. Wierzbowska, M. Lüders, and E. Tosatti, *J. Phys. B: At. Mol.*

- Opt. Phys. **37**, 2685 (2004).
- <sup>18</sup> L. Udvardi, AIP Conf. Proc. **544**, 187 (2000).
- <sup>19</sup> F. Uhlík, Z. Slanina, and E. Ōsawa, AIP Conf. Proc. **544**, 183 (2000).
- <sup>20</sup> K. Blum, *Density Matrix Theory and Applications*, (Plenum, New York, 1981).
- <sup>21</sup> G. D. Mahan, *Many-particle physics*, 3rd ed. (Kluwer, New York, 2000).
- <sup>22</sup> T. Kato *et al.*, Chem. Phys. Lett. **186**, 35 (1991); T. Kato, T. Kodama, and T. Shida, *ibid.* **205**, 405 (1993).
- <sup>23</sup> E. Tosatti, N. Manini, and O. Gunnarsson, Phys. Rev. B **54**, 17184 (1996), and references therein.